Geomorphology 192 (2013) 30–42

Contents lists available at SciVerse ScienceDirect

Geomorphology

journal homepage: www.elsevier.com/locate/geomorph

A scaling distribution for grain composition of debris flow

Li Yong [a,b,*], Zhou Xiaojun [a,c,d], Su Pengcheng [a,b,c], Kong Yingde [b,c], Liu Jingjing [a,b,c]

[a] Key Laboratory of Mountain Hazards and Surface Process, CAS, Chengdu 610041, China
[b] Institute of Mountain Hazards and Environment, CAS, Chengdu 610041, China
[c] University of Chinese Academy of Sciences, Beijing 100049, China
[d] China Merchants Chongqing Communications Research & Design Institute, Chongqing 400067, China

ARTICLE INFO

Article history:
Received 28 February 2012
Received in revised form 13 March 2013
Accepted 14 March 2013
Available online 23 March 2013

Keywords:
Grain composition
Scaling distribution
Distribution parameters
Debris flow

ABSTRACT

Debris flow is composed of a wide range of grains. This study proposes a general form of grain size distribution, $P(D) = CD^{-\mu}\exp(-D/D_c)$, which is satisfied well by various debris flows and by soils and sediments related to debris flows. The parameters μ and D_c are found to be related to debris-flow density in power laws. In particular, μ represents some characteristic porosity of soil in a natural condition and controls the variation of soils in developing debris flows; and D_c defines a characteristic size governing the sediment concentration. Field observations indicate that debris flows fall into a certain range of parameters (μ, D_c). Almost all debris flows have $\mu < 0.10$, and most debris flows of high density have $\mu < 0.05$. Moreover, experiments show that the exponent μ increases during soil failures under rainfall, providing an index varying in the course of debris flow initiation. Finally, grain size distribution is used to evaluate the properties of debris flows in different regions. The distribution provides a simple but quantitative method of predicting a potential flow through the source soils.

1. Introduction

Debris flow is composed of grains between 10^{-6} and 10^{0}m in size and differs much from either liquid or solid (Jaeger and Nagel, 1992). The widely used models of viscoplastic or Bingham flow (Johnson, 1970; Fink et al., 1981; Innes, 1983; Johnson, 1984; Nemec and Steel, 1984; Hiscott and James, 1985; Chen, 1988; Kim et al., 1995; Hutter et al., 1996; Jan and Shen, 1997) consider debris flow as a continuum fluid and ignore the effects caused by granular actions; for instance, the shear resistance generation, momentum transfer, and the detailed configuration of deposits (Iverson and Denlinger, 1987; Iverson, 1997). A comprehensive model of debris flow requires incorporating a variety of material rheologies (Hungr, 1995; Iverson and Vallance, 2001; D'Ambrosio et al., 2007). Though, the existing rheology in continuum models (e.g., Bingham fluid) is exclusively concerned with fine content up to clay-size grains (Julien and Lan, 1991; Iverson, 1997; Coussot and Ancey, 1999; Bardou et al., 2007; Chen et al., 2010), this does not really represent the nature of the matrix that incorporates coarse grains beyond the experimental capacity of rheology (Costa, 1984; Coussot and Meunier, 1996; Coussot, 1997; Kaitna et al., 2007). And no theoretical method is available for defining the boundary size distinguishing the grains constituting the matrix and the grains dispersed in the flow. Empirical estimates of such a size vary greatly between 0.06 and 20 mm (Kaitna and Rickenmann, 2007).

While fine grains govern the rheology, coarse grains are responsible for many macroscopic appearances of debris flow, such as the suspension of boulders on flow surface, the configurations of surge front, or the deposit lobes with steep and high strength margins of coarse clasts (Johnson, 1970; Fink et al., 1981; Innes, 1983; Nemec and Steel, 1984; Hiscott and James, 1985; Iverson and Denlinger, 1987; Kim et al., 1995; Iverson, 1997; Iverson and Vallance, 2001). Moreover, debris flow appears in many ways like granular flow and satisfies the criterions of shear flow (Bagnold, 1954, 1956; Batrouni et al., 1996). Numerical stimulation indicates that the grain aggregate forms a basal shearing layer in scale proportional to the variance of grain size (Campbell, 1989, 1990; Cleary and Campbell, 1993). A granular flow scenario incorporating grains in various sizes is expected to be more applicable for debris flow.

Grain composition as a whole is also crucial for initiation and developing of debris flow, as hydraulic properties of the soil depend on the grain size distribution (Arya and Paris, 1981; Hunt, 2004a,b; Nimmo et al., 2007). Evolving grain size distribution determines local mobility of flow, and grain size segregation is found to be crucial in flow transport and levee formation (Gray and Kokelaar, 2010; Johnson et al., 2012). Various forms of mathematical representations have been proposed (Cooke et al., 1993), including normal, log-normal, modified log-normal, log-hyperbolic, bi- or multimodal, and Weibull and Rosin–Rammler distributions (Gardner, 1956; Kittleman, 1964; Shirazi and Boersma, 1984; Campbell, 1985; Pinnick et al., 1985; Christiansen and Hartmann, 1988; Buchan, 1989; Wohletz et al., 1989; Wagner and

* Corresponding author at: Key Laboratory of Mountain Hazards and Surface Process, CAS, Chengdu 610041, China. Tel./fax: +86 2885238460.
E-mail address: ylie@imde.ac.cn (L. Yong).

0169-555X/$ – see front matter © 2013 Elsevier B.V. All rights reserved.
http://dx.doi.org/10.1016/j.geomorph.2013.03.015

Ding, 1992; Brown and Wohletz, 1995), but none of them is well applicable for debris flow. In addition, although the fractal feature appears in various soils (Turcotte, 1986; Perfect and Kay, 1991; Rieu and Sposito, 1991; Perfect et al., 1992; Buchan et al., 1993; Pachepsky et al., 2000; Hwang et al., 2002), no one single power law can cover the whole distribution (Avnir et al., 1985; Tyler and Wheatcraft, 1992; Pachepsky et al., 1995; Bittelli et al., 1999; Filgueira et al., 2003, 2006; Fu et al., 2009). In debris flow we have also found two scaling domains corresponding to the matrix and the coarse grains (Li et al., 2005), but no general form has ever been found for the wide-ranged grain composition.

In this paper we propose a general form of grain size distribution (GSD) for debris flows. The distribution is characterized by a couple of parameters defined by the grading analysis. The GSD parameters can be well related to debris flow properties in a natural way, and they constitute an initiation criterion of debris flow. Finally, we use the distribution to evaluate some debris flow events in various regions.

2. Sampling and measuring

Soil and sediment samples used in this study are collected from debris flow bodies and soils related to debris flows, including those of deposits, landslides, hillslopes, and glacial moraines in various geographic conditions.

Samples of debris flow bodies are collected in the Jiangjia Gully (JJG), a valley in west China, famous for the high frequency and variety of debris flow (Liu et al., 2008, 2009; Li et al., 2012). In JJG we have also collected samples from fresh and historic deposits of debris flows, from avalanches and landslides, and from soils on vegetated hillslopes (Fig. 1, in which numbers indicate sampling sites and A, B indicate the sites of slope failure and landslide). We also use samples from debris flow deposits in other valleys in Sichuan, Yunnan, Gansu, Liaoning, Beijing, and Tibet of China, collected by field surveys immediately after the occurrences.

Samples of flow bodies are taken by the cable-collector as the surge waves pass through the mainstream channel (Fig. 2); the flow density is directly measured. Other soils or sediments are randomly sampled for each case, following the conventional sampling methods (e.g., core and excavation methods).

The soil samples cover a range between 0.001 and 100 mm, which emphasizes the wide-ranged grains of debris. Granular analysis follows the soil classification criterion of USDA (Table 1). For simplicity, we call grains > 2 mm coarse, including the very coarse and gravel components. As an example, Table 2 lists the grain composition of a group of debris flow surges in JJG, in which the sizes in the first column are the lower limit sizes of gradation.

The granular analysis is conducted in traditional ways. Grains > 0.075 mm are sorted by sieve analysis, and grains below that are treated by hydrometer analysis based on sedimentary principle (Schofield and Wroth, 1968; Das, 2008). And for some samples, grains < 0.25 mm are measured by MS2000 laser particle size analyzer.

3. Grain size distribution of debris flow

3.1. General features of grain composition

Grain composition in debris flow generally presents a multimodal distribution (Fig. 3, using data in Table 2). Curves in Fig. 3 reveal that the flow density decreases as the peak of the coarse content lowers and moves from left (fine) to right (coarse). Besides the peaks at fine and coarse content, also appear intermediate peaks, of which the effects are ambiguous. In practice, some special sizes and their combinations, such as the uniform coefficient ($C_u = D_{60} / D_{10}$) and gradation coefficient ($C_c = D_{30^2} / D_{10}D_{60}$), are used to describe the grain composition. However, these indices are somewhat arbitrarily defined and cannot specify the whole distribution.

Although many cumulative curves have been proposed for grain size distribution (GSD) in soil studies, no general representation is

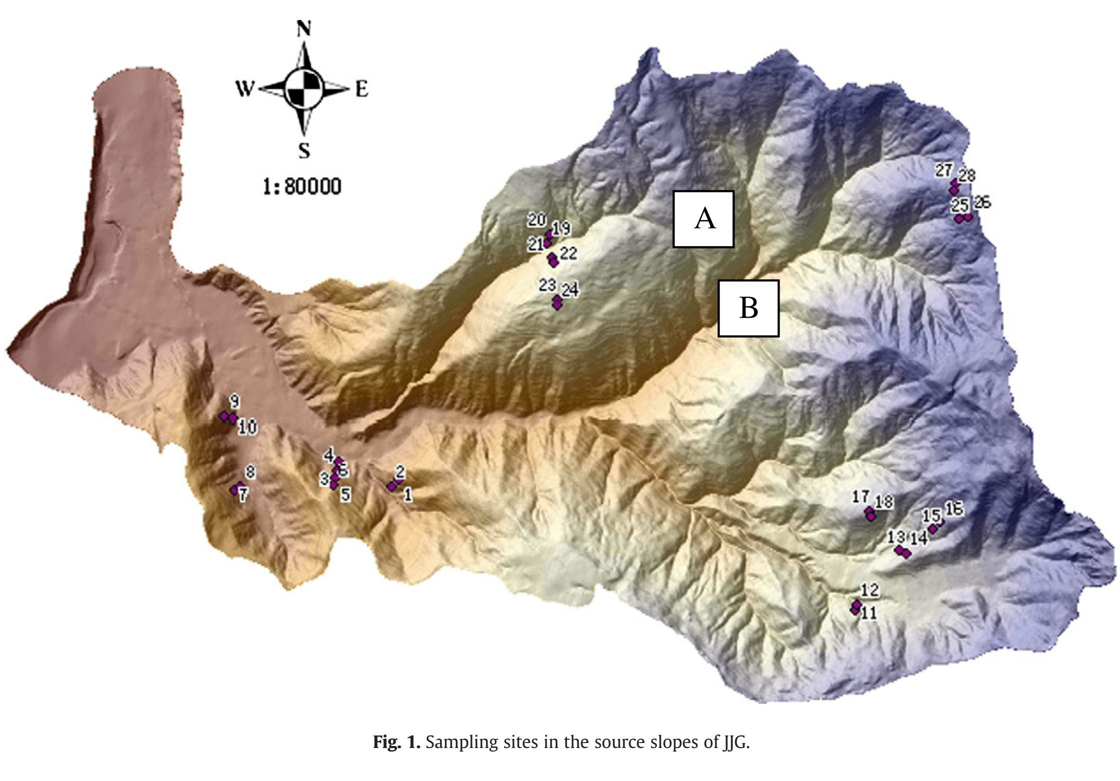

Fig. 1. Sampling sites in the source slopes of JJG.

Fig. 2. Sampling of living debris flow surge in JJG.

available for the wide-ranged grain composition. We have found fractal regimes existing in the fine and coarse content (Li et al., 2005); but for the composition as a whole, the exponential function seems to fit better:

$$P(D) = C\exp(-kD) \tag{1}$$

where $P(D)$ is the percentage of grains $> D$ (mm) and k is a coefficient. Fig. 4 shows the $P(D)$ curves in Fig. 3. The exponential function derives a characteristic diameter defined by $D_c = 1/k$. Rescaling grain size by D_c, the curves collapse almost on the same single exponential curve, as shown in Fig. 5, which contains 34 soil samples of debris flows in JJG.

Moreover, D_c characterizes the bulk property of flow, which varies with flow density in a power law (Fig. 6),

$$\rho \sim k^{-n} \text{ or } \rho \sim D_c^n \left(R^2 = 0.86\right). \tag{2}$$

But discrepancy appears still at low densities or fine grains (white points in Fig. 6), suggesting that the exponential distribution does not hold well in general. A more general distribution is thus required.

3.2. A general form of grain size distribution

Noting that the fractal holds for fine grains while exponential function fits the coarse grains well, we try to propose a distribution incorporating both of them, i.e.,

$$P(D) = CD^{-\mu}\exp(-D/D_c). \tag{3}$$

Here, μ is a power exponent, and D_c is the characteristic size as defined above. This form of GSD turns out perfect for various soil samples related to debris flows.

Table 1
Classification of soil (USDA) (unit: mm) (Das, 2008).

Gravel	Very coarse sand	Coarse sand	Medium sand	Fine sand	Very fine sand	Silt	Clay
>2	2–1	1–0.5	0.5–0.25	0.25–0.1	0.1–0.05	0.05–0.002	<0.002

3.2.1. GSD of debris flow

Then we use Eq. (3) for grains of debris flow. Table 3 lists the parameters for a surge group of a debris flow in JJG (also including the data in Table 2), with $R^2 \sim 1$ for almost all cases.

The high goodness can be presented more conspicuously by rescaling both the grain size and the cumulative fraction. If we rewrite Eq. (3) as

$$P(D)D^{\mu}/C = \exp(-D/D_c) \tag{4}$$

and rescale the grain size by D_c, then all the distribution curves collapse onto the single scaling function $G = \exp(-D/D_c)$, and for this reason we call GSD (Eq. (3)) the scaling distribution (Fig. 7, containing all samples in Table 3).

More examples satisfying the distribution are listed in Tables 4 and 5, respectively for a surge group in a single event (in 1975) and a random set of surges from various debris flows in JJG.

Table 2
Grain composition of debris flows.

Size (mm)	Grain composition							
	S1	S2	S3	S4	S5	S6	S7	S8
80	–	–	–	4.4	–	–	–	–
40	–	2.98	17.04	14.01	7.76	17.84	13.65	8.69
20	–	4.18	20.37	19.07	14.65	13.68	19.74	16.97
10	0.38	1.81	5.45	7.09	8.43	7.55	9.84	8.12
7	0.4	5.74	7.88	6.76	7.05	8.96	6.43	7.2
5	1.33	11.59	8.41	8.15	11.38	5.07	8.22	16.36
3	22.86	19.5	4.5	4.16	6.78	4.61	4.18	0.26
2	17.86	1.62	4.22	4.78	4.52	3.18	3.35	3.66
1	6.12	3.38	2.2	2.12	5.5	3.97	2.82	5.27
0.5	6.67	4.53	2.21	2.4	3.46	1.91	2.28	2.8
0.25	7.28	5.87	2.33	2.43	3.6	2.32	2.88	4.3
0.1	3.6	4.06	2.36	1.67	2.24	2.42	1.73	2.82
0.05	15	16	5.6	7	8.1	11	7.8	13.8
0.01	9.3	10.2	9	9	12	3.2	6.2	5
0.005	2.8	3	3.3	3.2	1.4	1.2	0.8	1.5
0.001	2.9	2.8	1.7	1.8	2.1	1.6	1.2	1.7
Density (g/cm^3)	1.57	1.83	2.10	2.17	2.00	2.20	2.21	2.09

Note: sizes in the first row are the lower limit of the size range.

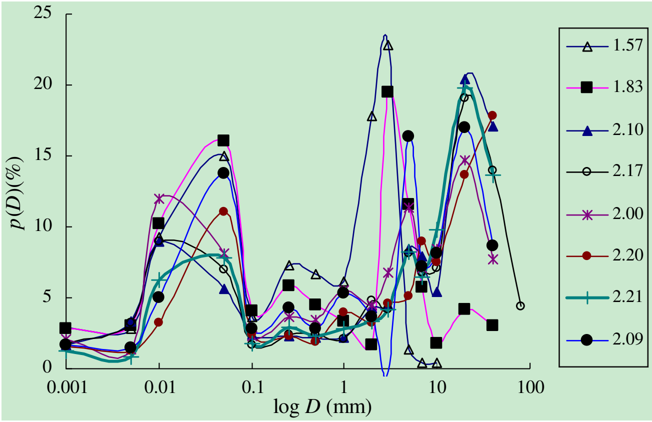

Fig. 3. Grain composition of debris flow with different densities.

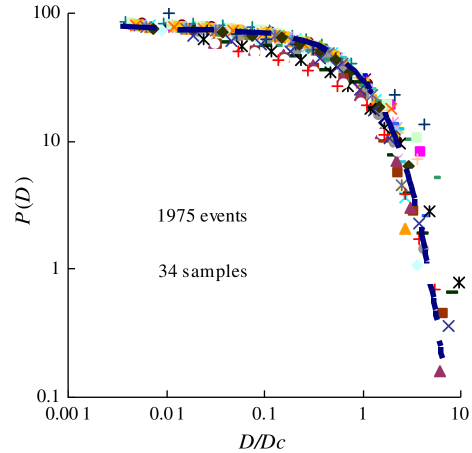

Fig. 5. Rescaled exponential distribution of grain size of debris flow.

And relationships turn out to hold between GSD parameters. At first, we find that the coefficient C is related to exponent μ in definite manners. As shown in Fig. 8, the μ–C relationship appears in the form of linear or exponential function. Despite the variety of the forms, the existence of specific relationship suggests that the coefficient is not an independent variable. Then the distribution is principally determined by μ and D_c. More importantly, both μ and D_c are related to the flow density by a power law. Figs. 9 and 10 display the relationships of GSD parameter to flow density for different samples of debris flows (using data in Tables 3 and 5).

$$\mu \sim \rho^{-m} \text{ and } D_c \sim \rho^{-n}. \tag{5}$$

3.2.2. GSDs of source and deposits of debris flows

Discussions above are concerned with living debris flow surges. But in practice, it is hardly possible to catch a moving debris flow. In most cases, we can only get samples from the source soils or deposits left by flows, which should be much different from flow materials because changes have taken place during the processes from source soils to flows and from flows to deposits. Then we'd better examine whether the GSD of Eq. (3) is applicable or not for these cases.

At first, we use the GSD to fit the slope soil, landslide soil and debris-flow deposit soil, randomly taken from JJG. The result proves well, with parameters and goodness of fit listed in Table 6.

Then we take soils from a potential landslide at different depths (from 15 to 90 cm). The grain composition varies remarkably with depth. Coarse content (>2 mm) is about 40% between 60 and 75 cm and 62% for others; fine content (<0.1 mm) is about 3% between 15 and 45 cm and 10% for others (Wu et al., 1990). However, all the soils conform to the expected GSD (Table 7).

For more convincing confirmation of the GSD, we consider a huge historical deposit plateau in the south of JJG, estimated between 12,000 and 18,000 years according to Carbon-14 dating (Wu et al., 1990). This deposit is distinct from the fresh deposit in appearances and grain composition; but the soils present the same GSD, as shown in Table 8, which contains four samples (An1–An4), with a perfect linear μ–C relationship of $\mu = -0.055C + 0.55$ ($R^2 = 0.99$).

Note that the distinction here relies in parameters μ and D_c. The values of μ and D_c are relatively greater than those of debris flows, reflecting the fact that the grain composition, especially the fine

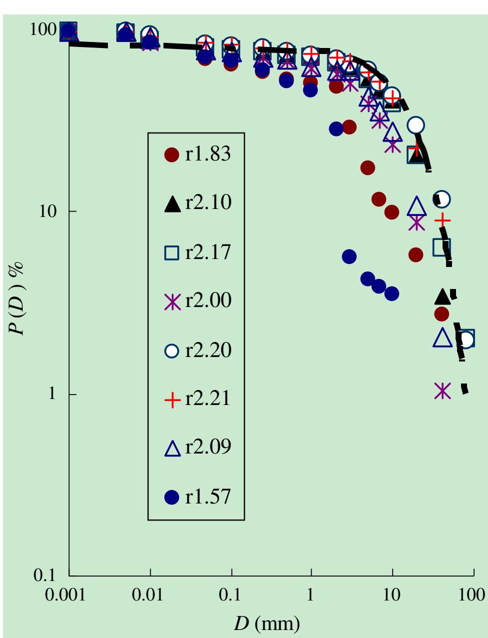

Fig. 4. Exponential distribution of grain size of debris flow.

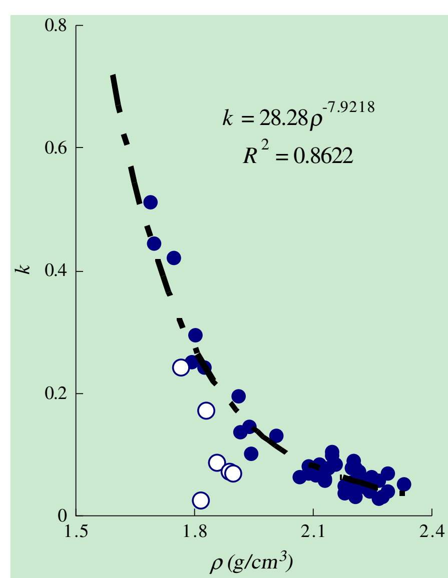

Fig. 6. Distribution parameter varying with debris-flow density.

Table 3
GSD parameters for a surge group of debris flow (1974).

Sample	Density ρ (g/cm^3)	Coefficient C	Power index μ	Characteristic size D_c (mm)	R^2
1	1.567	61.62	0.0691	2.2538	0.9886
2	1.83	56.29	0.0850	6.0827	0.9818
3	1.841	59.83	0.0750	9.0580	0.9880
4	2.101	74.48	0.0380	17.8731	0.9946
5	2.168	72.89	0.0418	18.8679	0.9954
6	1.995	68.96	0.0556	11.1607	0.9955
7	2.077	72.40	0.0476	17.7462	0.9926
8	2.204	75.87	0.0405	23.0733	0.9960
9	2.210	78.10	0.0364	27.4801	0.9953
10	2.25	80.07	0.0326	28.6944	0.9961
11	2.164	70.65	0.0501	13.9860	0.9933
12	2.251	76.09	0.0385	16.6834	0.9933
13	2.074	70.77	0.0506	16.0643	0.9942
14	2.19	76.81	0.0377	21.1999	0.9925
15	2.206	78.44	0.0342	19.1022	0.9963
16	2.186	76.90	0.0392	20.2429	0.9960
17	2.090	69.39	0.0538	13.1062	0.9918
18	2.206	77.21	0.0375	24.2777	0.9974

content, has been changed greatly by rainfall and water flow after the deposition.

3.2.3. GSDs for soils on vegetated slopes

As the distribution applies well to debris flows and to the related soils, one may wonder whether it applies to other soils in natural conditions. For this we consider soils from the vegetated slopes in JJG (with sites shown in Fig. 1), which are not necessarily the source of debris flow. The result is satisfactory only with considerable fluctuation of the parameters (Table 9, with all $R^2 \sim 1$ omitted), and a robust μ–C relationship also appears (Fig. 11).

3.2.4. GSD for debris flows in general

Although the scaling GSD is derived from soil samples in JJG, we find that it generally holds for debris flows in other valleys. Fig. 12 shows the GSDs of debris flow deposits from 27 gullies in the upper Yangtze, with samples collected by the authors immediately after the occurrences.

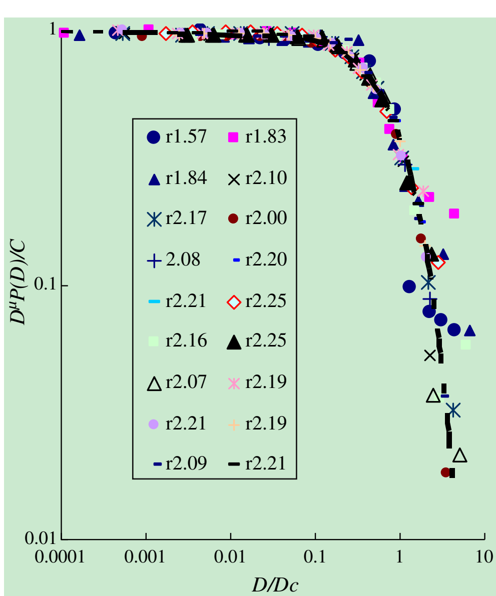

Fig. 7. The rescaled scaling distribution of grains of debris flow.

Table 4
GSD parameters for a surge group of debris flow (1975).

Sample	Density ρ (g/cm^3)	Coefficient C	Power index μ	Characteristic size D_c (mm)	R^2
1	2.206	77.33	0.03053	23.67985	0.9986
2	2.21	74.98	0.04522	28.06624	0.9916
3	2.19	75.53	0.03396	21.42704	0.9977
4	2.202	76.96	0.01792	15.93625	0.9986
5	2.221	75.77	0.03439	23.44666	0.9985
6	2.202	78	0.0232	20.21427	0.9997
7	2.292	82.71	0.01615	29.22268	0.9994
8	2.213	77.1	0.02844	24.42599	0.9992
9	2.211	76.68	0.02381	20.34174	0.997
10	1.947	66.29	0.04291	13.87347	0.9986

And the GSD also fits debris flows in various regions of China, including Beijing, Yunnan, Tibet, Sichuan, and Gansu, the provinces frequently suffering from debris flows (Table 10). We note that even such a set of data from diverse sources presents a definite μ–C relationship, a power law with exponent of −4.0 (Fig. 13).

3.3. GSD parameters and debris flow properties

Then we find that the scaling distribution holds generally for debris flows; the distinction relies only in the parameters (μ, D_c). As shown in Fig. 14, the (μ, D_c) points cluster in distinct groups, respectively representing vegetated slope soils, landslide soils, ancient deposits, and different debris flow events.

We note that, compared with the points of landslide and the scattering points of ancient deposit (white triangles), debris flows fall into a certain range of parameter values. Apparently small μ is most favorable for debris flow; most flows have $\mu < 0.10$; and many of them have $\mu < 0.05$.

Accordingly, a working criterion can be drawn from debris flows in JJG (Table 11). As rough as it may be, such a criterion is practically helpful in evaluating debris flow by GSD of soils, as in most cases we have no further information about the living flow but only have data of the deposits or the source soils.

4. Physical meanings of the GSD

So we have confirmed the universal validity of the scaling GSD for various debris flows. In the following we try to work out the physical meaning of the distribution and find its implication in debris flow initiation. At first, the distribution suggests the existence of some underlying principle of grain aggregating in a natural condition. For example, the exponential component may find its root in the repulse

Table 5
GSD parameters for a random set of debris flow surges in JJG.

Samples	ρ_c (g/cm^3)	C	μ	D_c (mm)	R^2
1	1.30	11.49	0.3067	0.2124	0.9961
2	1.34	13.84	0.2462	6.9109	0.9818
3	1.48	16.27	0.2489	1.2276	0.9965
4	1.65	38.34	0.1198	2.4624	0.9946
5	1.74	31.73	0.1522	2.5349	0.9975
6	1.81	57.49	0.06792	8.6505	0.9971
7	1.91	62.26	0.05635	16.4393	0.9984
8	1.99	70.51	0.04336	16.6058	0.9965
9	2.01	57.34	0.06471	8.3752	0.9942
10	2.08	70.79	0.03963	16.6528	0.9975
11	2.16	79.65	0.02643	26.8673	0.9984
12	2.18	77.94	0.02914	23.9751	0.9970
13	2.22	78.83	0.02780	31.2402	0.9962

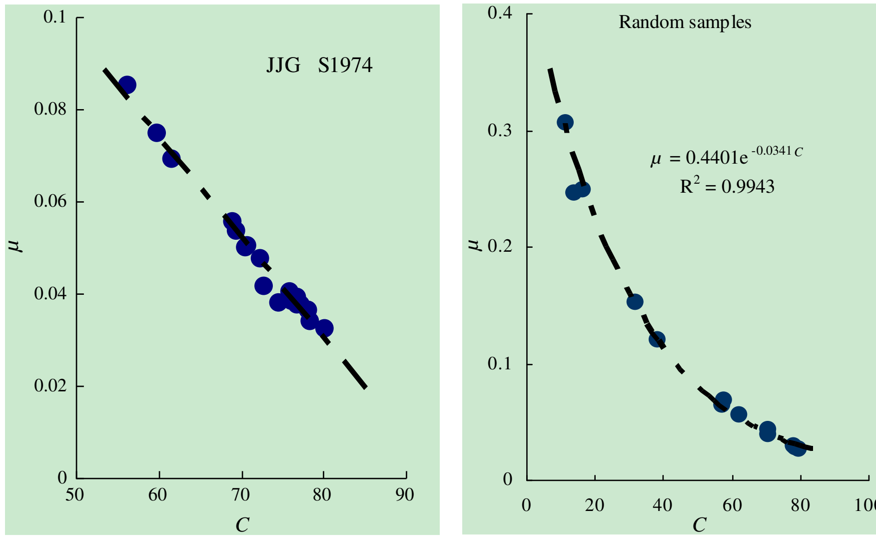

Fig. 8. μ–C relationship of the GSDs.

potential of grain (Das, 2008). This goes beyond the scope of the present discussion, but it is an intriguing issue worthy of further studies. We can reasonably assert that the distribution holds in general and that the variation of parameters should be related to the soil behavior. For the present, we consider only the soil behavior following the variation of parameters.

4.1. Meaning of the exponent

Grain aggregation in natural conditions always abounds with pores of various sizes; therefore the distribution of grain size implies an associated distribution of pore size. Because pores dominate in fine content, we consider the fine content in the composition. For fine grains, $D \ll D_c$ or $\exp(-D/D_c) \sim 1$, the distribution reduces to a power law:

$$P(D) \sim D^{-\mu}. \tag{6}$$

This implies that the fine grains form a fractal, which also leads to a fractal of pore in proportion to the grain size (Arya and Paris, 1981; Gevirtzman and Roberts, 1991; Hunt and Gee, 2002; Hunt, 2004a). In terms of percolation in porous media (Katz and Thompson, 1985; Rieu and Sposito, 1991; Hunt, 2004b), the total porosity, σ, can be estimated by

$$\sigma = 1 - q^{\mu} \tag{7}$$

where $q = (D_0/D_m)$, D_0 and D_m are, respectively, the lower and upper limits of the fractal range. As sampling and granular analysis may change the porosity, the estimated porosity should be taken as the characteristic porosity in natural conditions. In other words, different GSD parameters correspond to different porosities.

Since $D_0/D_m < 1$, σ is a monotonous increasing function of μ, meaning that a big exponent μ represents a high porosity. For an intuitive example, consider $D_0 \sim 0.002$ mm, the upper limit size of clay grain, and $D_m \sim 2$ mm, the estimated maximal size of the matrix (e.g., Fei and Shu, 2004). This defines $q \sim 0.002/2 = 0.001$. Taking $\mu = 0.05$ and 0.15 as the typical values for debris flow and deposit respectively (cf. Tables 3, 4, and 5, Fig. 14), we have porosity $\sigma = 1 - q^{\mu} = 0.30$

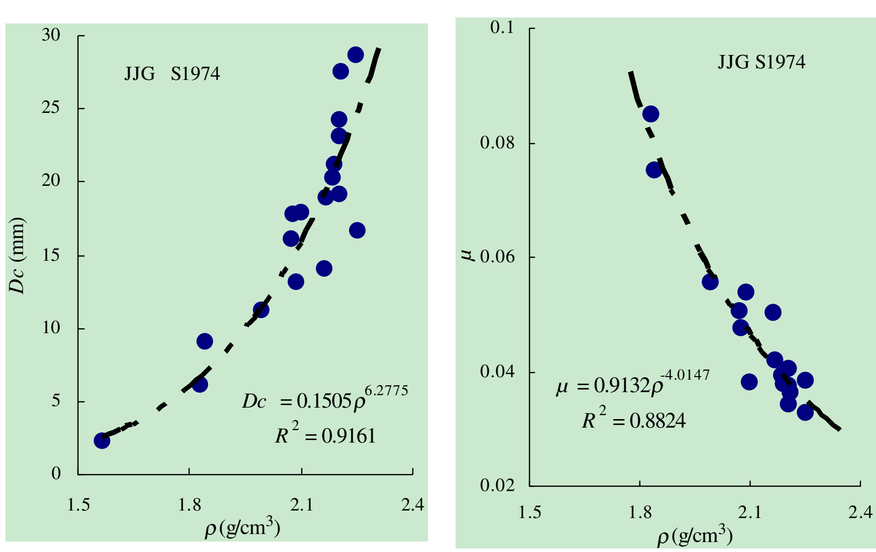

Fig. 9. Relationship between density and GSD parameter (1974).

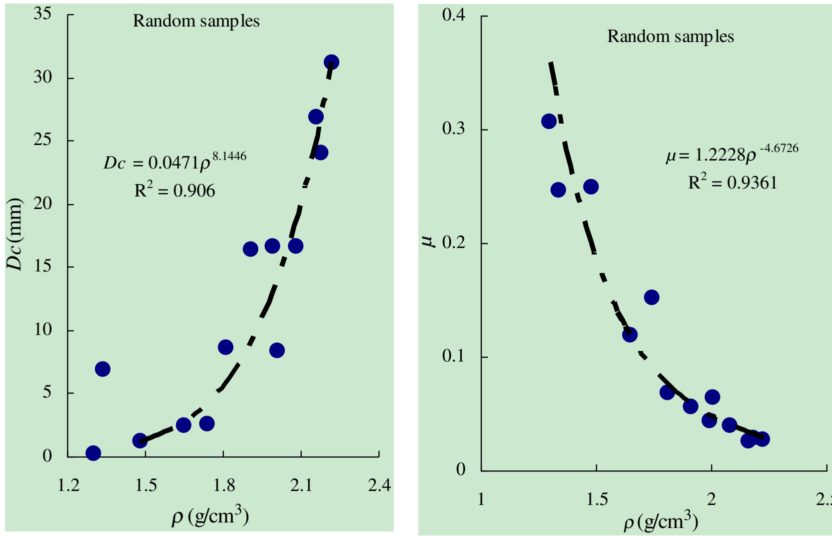

Fig. 10. Relationships between GSD parameters (for random samples).

and 0.65, rightly corresponding to the sediment concentration for observed debris flows. Taking the grain density as 2.65 (g/cm^3), we get the flow density of 2.16 and 1.58 (g/cm^3), which agrees well with the observed values. Thus the exponent μ provides a simple, direct, and intuitive index of the porosity.

The exponent can be further determined through the critical criterion for granular flow. Obviously, μ is also associated with grain concentration by $C = q^{\mu}$ as $C = 1 - \sigma$. Grain concentration relies in the manner of grain packing. A grain aggregate may achieve an ideal concentration (corresponding to the most compact packing). For hexagonal compact packing, C is 0.74; and for uniform sphere (random close packing), it is 0.64 (Aste et al., 2007). For an aggregate of grains in a wide range of sizes, the concentration might be much higher because of the effects of fine-grained pore filling. A grain aggregate with high concentration requires strong shearing stress to initiate. According to Bagnold (1954, 1956), a critical concentration is required for shearing. Using the linear concentration λ introduced by Bagnold, we have

$$1/\lambda = (C_0/C)^{1/3}-1 \text{ or } C/C_0 = (\lambda/(1+\lambda))^3. \tag{8}$$

Because $C = q^{\mu}$ (Eq. (7)), it yields

$$q^{\mu/3} = k\lambda/(1+\lambda) \tag{9}$$

where $k = C_0^{1/3}$. Then the exponent μ reduces to a function of λ, k, and q,

$$\mu(\lambda, k, q) = 3\ln(k\lambda/(1+\lambda))/\ln q. \tag{10}$$

Because $k = C_0^{1/3} = 0.90$ and varies little (e.g., $k = 0.96$ when $C_0 = 0.90$, an extreme concentration), μ depends mainly on λ and q.

Using the critical λ = 22 for shearing flow (Bagnold, 1954), Eq. (10) yields

$$\mu(q) = 3\ln(0.9\times 22/(1+22))/\ln(q) = 0.45/\ln(D_m/D_0) \tag{11}$$

(here note that appearing in the denominator is 1 / q because of multiplying by a minus derived from the numerator.) Although the linear concentration derives from uniform spherical grains in Bagnold's experiments, the critical concentration should be useful in general. The threshold value λ = 22 corresponds to a grain concentration of $C = 0.70$ (using $C_0 = 0.80$ for the grains of debris flow), which coincides well with the observed data of debris flows.

Eq. (11) indicates that the exponent μ is sensitive to the fractal domain defined by D_m / D_0 (cf. Eq. (7)). For the case considered above, q ~ 0.001 has $\mu = 0.06$, and q ~ 0.01 has $\mu = 0.10$, in good agreement with the observed values for debris flows. Since dμ / dλ = 3 / (1 + λ) ln$q$ < 0, μ decreases monotonically with λ (Eq. (10)). This means μ (λ < 22) > μ (λ = 22), and therefore Eq. (11) defines the lower limit

Table 6
GSDs for different soils concerning debris flow.

Soil	C	μ	D_c (mm)	R^2
Landslide	67.24	0.0544	18.4332	0.9963
Slope	72.37	0.05129	18.6463	0.9759
Deposit	76.04	0.03971	23.3154	0.9947

Table 7
GSDs of landslide soils at different depths on a slope in JJG.

Soils	C	μ	D_c (mm)	R^2
S15	51.42	0.1369	2.6824	0.9923
S30	67.80	0.1312	8.3682	0.9793
S45	106	0.2206	1.9467	0.983
S60	52.91	0.1797	11.0522	0.9863
S75	77.43	0.06842	14.3266	0.9927
S90	66.35	0.1107	5.2715	0.9874
S_{av}	63.90	0.1283	7.7042	0.9856

Table 8
GSDs for deposits of historical debris flows in JJG.

History	Samples	C	μ	D_c (mm)	R^2	Year (10^4 a)
Ancient	1	63	0.1815	27.9252	0.98	
	2	58	0.2272	33.1455	0.99	1.70
	3	65.93	0.1681	22.3764	0.99	1.45
	4	70.08	0.1441	24.6427	0.99	1.20
Old	5	73.25	0.1248	48.8043	0.98	
Modern	6	89.69	0.03755	81.4332	0.98	

Table 9
GSD parameters for vegetated soils in JJG.

Group	Sample	C	μ	D_c (mm)
A	1	73.86	0.04272	5.7471
	2	68.63	0.05425	8.8810
B	3	70.51	0.04760	9.3985
	4	81.57	0.02403	4.9652
	5	87.63	0.01430	12.9366
	6	85.80	0.01673	10.3993
C	7	50.37	0.08660	15.0512
	8	49.89	0.08309	14.3864
	9	66.48	0.05463	7.0922
	10	69.05	0.05083	9.8619
D	11	62.32	0.05495	22.4115
	12	45.62	0.09785	12.3213
E	13	47.01	0.09846	12.6486
	14	44.61	0.01009	13.8658
	15	41.14	0.1180	13.7950
	16	36.63	0.1312	11.6973
	17	69.83	0.04615	15.1906
	18	68.84	0.04636	13.2503
F	19	54.10	0.08192	9.7847
	20	69.51	0.04287	9.3458
	21	56.60	0.06896	8.0710
	22	59.98	0.06197	8.3195
	23	60.62	0.05490	6.2500
	24	67.28	0.04208	8.9206
G	25	48.85	0.09872	16.8919
	26	63.73	0.05702	13.8122
	27	63.05	0.05718	10.0110
	28	67.34	0.04918	11.9832

of μ. It follows that an aggregate of high concentration (high C) has a small exponent μ while that of low concentration has a high exponent.

4.2. Meaning of the characteristic grain size

Because μ decreases with D_m / D_0 (Eq. (11)), this means the porosity decreases with D_m / D_0. Then the concentration increases with D_m / D_0. On the other hand, since the flow density (hence the concentration) increases with D_c, D_m / D_0 should also increase as D_c. Because D_m / D_0 defines the fractal range of grains and controls the initiation of flow, we can take the range as constituting the matrix of debris flow, and thus D_m defines an upper limit of grains of the matrix. Shortly speaking, a soil with big D_c has a big D_m, and hence a low porosity and a high concentration. This implies that debris

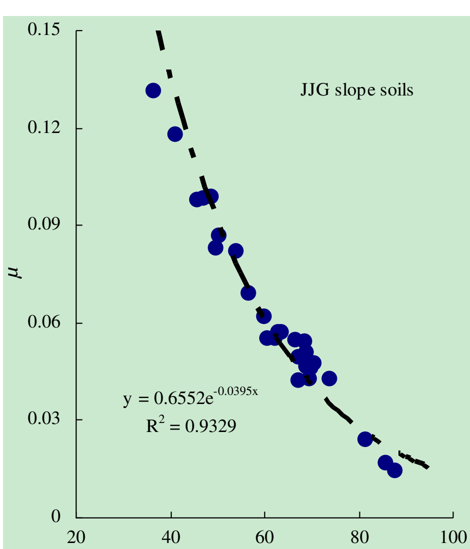

Fig. 11. μ–C relationship for vegetated slope soils in JJG.

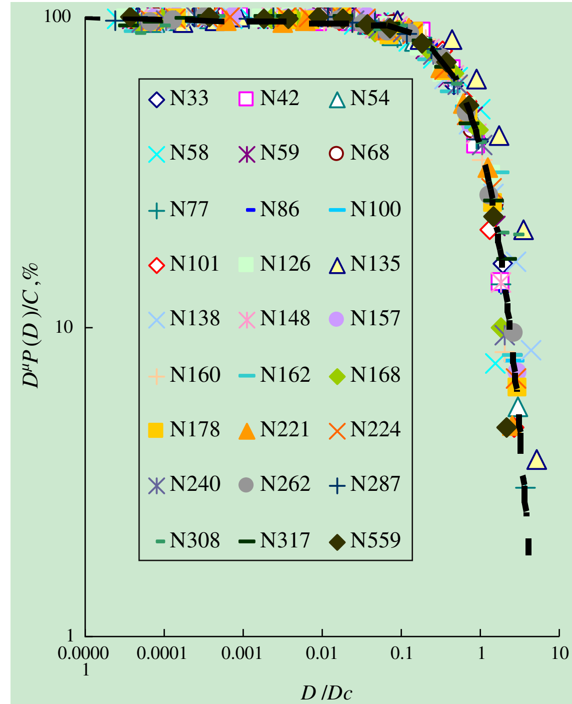

Fig. 12. GSDs for debris flow samples of the Upper Yangtze.

Table 10
GSDs for debris flows of valleys in various regions.

Valleys	Sample	C	μ	D_c (mm)	R^2
Ketai Beijing	K1	86.69	0.02386	226.2955	0.9921
	K2	97.64	0.01056	94.69697	0.9894
	K3	83.70	0.03167	68.21282	0.9906
	K4	64.34	0.06968	10.80847	0.9757
Lulang Tibet	L1	77.24	0.04587	25.6410	0.9941
	L2	85.85	0.03106	24.4738	0.9816
	L3	122.8	0.03586	0.5051	0.9908
	L4	64.07	0.08764	15.2369	0.9164
	L5	101.5	0.004814	31.8573	0.9349
Huoshao Gansu	F1	46.5	0.2029	28.2406	0.9314
	F2	65.12	0.102	61.3874	0.9833
	F3	62.57	0.1148	20.1369	0.9868
Midui Tibet	M1	88.7	0.02153	7.3692	0.9908
	M2	85.65	0.03002	7.2727	0.0885
	M3	86.63	0.02914	43.2900	0.0030
	M4	90.71	0.02109	42.7533	0.9905
	M5	81.43	0.01915	27.7855	0.9901
	M6	84.43	0.02902	25.1319	0.9985
Guonai Tibet	G1	73.32	0.05054	11.7261	0.9752
	G2	91.95	0.01608	70.9220	0.9941
	G3	97.15	0.005526	103.4340	0.9985
Heishui Yunnan	H1	87.47	0.02096	12.6839	0.9923
	H2	83.75	0.02749	19.0621	0.9940
	H3	95.91	0.007721	5.7904	0.9987
	H4	68.84	0.04888	14.3843	0.9960
	H5	103.8	0.01115	12.7502	0.9961
Weijiagou Sichuan	W1	98.96	0.002606	11.5327	0.9985
	W2	100.6	0.01495	13.3333	0.9915
	W3	93.24	0.01977	11.4090	0.9976
	W4	94.61	0.002608	12.4008	0.9970
	W5	101.8	0.01915	12.0005	0.9971
Luojiayu Gansu	Lu1	92.83	0.02209	26.1164	0.99915
	Lu2	90.93	0.02893	13.7155	0.99765
	Lu3	90.32	0.04023	12.6839	0.99936
	Lu4	99.44	−0.00701	13.1613	0.99656

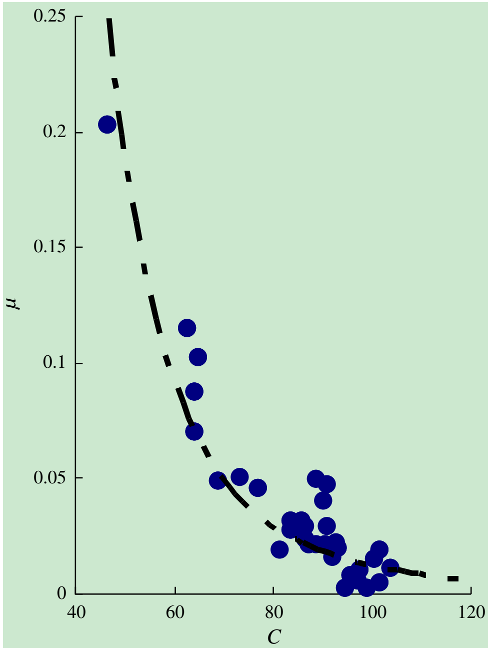

Fig. 13. μ–C relationship for debris flows in different valleys.

Table 11
Relationship between debris-flow properties and GSD parameters.

Flow nature	ρ (g/cm^3)	C	μ	D_c (mm)
Concentrated flow	1.2–1.5	10–20	0.20–0.30	<2
Low-density debris flow	1.6–1.9	30–60	0.05–0.10	2–15
High-density debris flow	>2.0	60–80	<0.05	>15

flow with ever-increasing D_c may assimilate more coarse grains into the matrix and thus increase the energetic power and transport capacity. This can be confirmed by debris flows in JJG. According to our observations, the sediment volume transported by debris flow increases with D_c in a power law manner, $S \sim D_c^{0.32}$ (Fig. 15), which is just parallel to the power-law relation of $C = q^{\mu} = (D_0 / D_m)^{\mu}$.

Then we see that the parameters μ and D_c respectively describe the fine and coarse content of the grain composition. A small exponent μ implies a high concentration of grain and high density of flow; and the grain size in matrix increases with D_c, which leads to a high concentration and transport capacity of debris flow. This provides an explanation for the observed facts in Table 11.

5. Experiments for parameter variations

From source soils to moving surges, grain composition in debris flow undergoes constant changes. In order to see the changes of GSD parameters, we have conducted a series of experiments simulating soil failures under artificial rainfall of different intensities, durations, and slope gradients (Zhou et al., 2012). The soils are collected from the debris flow caused by the Wenchuan earthquake on 12 May, 2008, and the soils used in experiments have the original GSD parameters of $\mu = 0.013$ and $D_c = 22.03$ (mm).

During the rainfall, the soils collapsed and accumulated at the slope foot, which then turned into debris flow. We found that the accumulated failure soils retain the same GSD, only with the exponent μ increasing remarkably, up to one order of magnitude (Table 12).

The observed increase of μ was accompanied by the loss of fine content with infiltration of water. As fine grains loss, the porosity increases. This again confirms that μ represents the porosity in natural conditions (Eq. (7)). This plays a crucial role in debris flow initiation. When soil gets high porosity it will contract and begin to shear; the contraction may increase the pore water pressure and reduce the frictional strength and finally result in liquefaction (Iverson et al., 2000). On the other hand, if the porosity is much higher at first, say, $\mu > 0.10$, the soil would be dominated by the intermediate fluid and start to flow before it can form a cohesive aggregate. Therefore, soils with high exponent usually form low density debris flow or hyperconcentrated flow.

The experiments also indicate that the same soils may result in debris flow of different grain compositions, depending on the intensity and duration of rainfall. As seen from Table 12, the μ value varies between about 0.003 and 0.10, covering the full spectrum of debris flows (cf. Table 11 and Fig. 14), meaning that the resulted flows might take different flow regimes.

Therefore, the exponent μ not only represents the porosity but also provides an index describing the variation of grain compositions in the developing of debris flow.

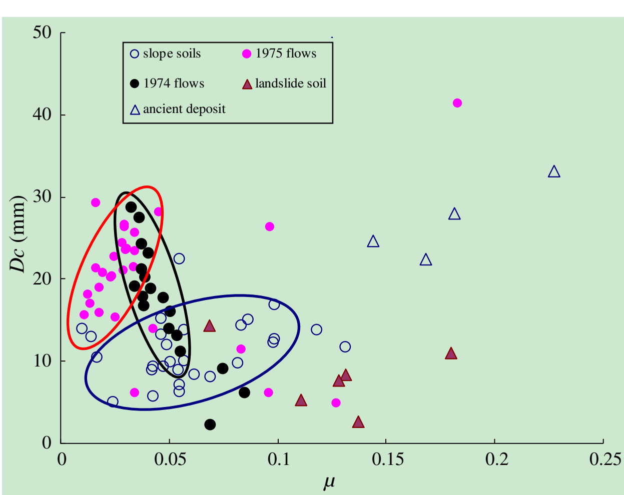

Fig. 14. Soil groups identified by GSD parameters.

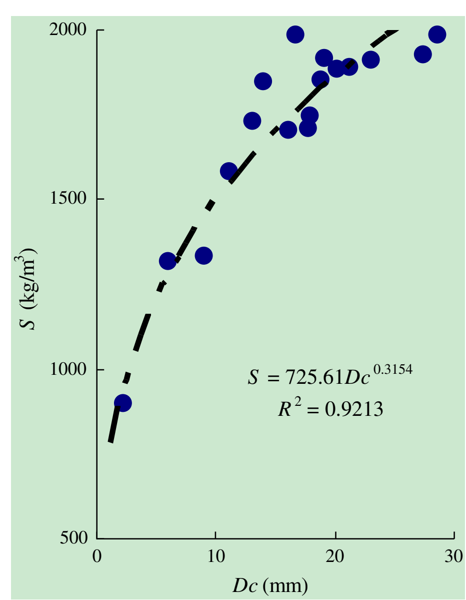

Fig. 15. Relationship between sediment concentration and characteristic grain size.

Table 12
GSD parameter variations under artificial rainfalls.

Test run	Rainfall (mm/h)	Duration	Slope gradient	GSD parameters		
		(min)	(degree, °)	μ	D_c (mm)	R^2
1	53	10	10.74	0.1124	12.42	0.984
2		20	16.74	0.05143	8.51	0.997
3		30	22.94	0.0372	9.50	0.9988
4		50	30.56	0.0717	9.83	0.9914
5	119	10	22.94	0.061	19.81	0.9957
6		20	30.56	0.048	13.3	0.9976
7		30	10.74	0.0167	10.27	0.9966
8		50	16.74	0.0438	12.41	0.9984
9	198	10	16.74	0.0544	10.59	0.9968
10		20	10.74	0.0377	9.15	0.9965
11		30	30.56	0.0268	8.84	0.9965
12		50	22.94	0.0187	8.03	0.9986
13	292	10	30.56	0.1058	7.16	0.9954
14		20	22.94	0.0517	16.8	0.9944
15		30	16.74	0.0446	13.99	0.9945
16		50	10.74	0.0668	22.64	0.9974
Original soil				0.0132	20.10	0.9987

6. Application of GSD in debris flow assessment

Because of its universal validity, the scaling GSD can be used in debris flow assessment. In particular, the criterions in Table 11 may be used to identify flow properties by their GSD parameters. In the following, we apply the GSDs to groups of debris flows in recent years in west China.

The events include (i) debris flows in the areas hit by the Ms8.0 earthquake on 12 May, 2008, in Wenchuan, Sichuan, southwest China (Cui et al., 2011; Su et al, 2011); (ii) a group of devastating debris flows in Zhouqu, Gansu, northwest China (Hu et al., 2010; Yu et al., 2010; Tang et al., 2011); and (iii) debris flows in the last rainy season (July to September 2012) in Sichuan. For each occurrence, we have carried out field surveys, collected soil or sediment samples from the source areas and deposits, and conducted granular analysis in conventional ways. Tables 13 and 14 listed the GSD parameters and Figs. 16 and 17 display the (μ, D_c) points.

Apparently, the GSD parameters fall into the same ranges as those we set for debris flows in JJG (Table 11; Fig. 14); and at the same time, they are also distinct from one another on a valley or regional scale. For example, several groups can be identified in Fig. 16, distinguishing between Luojiayu and Sanyanyu in Gansu and others in Sichuan. The characteristic D_c indicates that grains in Sanyanyu are much coarser than Luojiayu, in agreement with our field observations. And the exponent μ indicates that debris flows in the Beichuan–Ningqiang area are mostly high density while in Pengzhou–Mianzhu they vary between high and moderate density.

It follows that the GSD parameters can not only identify the properties of single debris flow, but also reflect the varieties of debris flows. They distinguish debris flows in different regions or valleys and characterize variation of debris flows in a certain valley.

7. Conclusions and discussions

Granular material of debris flow follows the grain size distribution of $P(D) = CD^{-\mu}\exp(-D / D_c)$. The parameters μ and D_c are naturally determined by granular analysis. For fine grains, the distribution reduces to the power law with exponent μ, which represents the porosity of grains. Observations indicate that debris flow density decreases with μ and increases with D_c in power law forms. Moreover, following the critical condition of shearing flow of granular materials, we derive the critical value of the exponent μ, which agrees well with

Table 13
GSD parameters of debris flows in Wenchuan and Zhouqu.

Gullies	Gullies	County or location	C	μ	D_c (mm)
Area of the Wenchuan Earthquake, 2008-05-12	Chapinghe	Anxian	79.35	0.05	15.18
	Zhangjiawan	Beichuan	90.28	0.02	26.41
	Shaoyao	Mianzhu	81.06	0.043	11.83
	Tributary Qizu	Ningqiang	93.75	0.011	25.22
	Lower Qizu		86.25	0.029	34.19
	Shijiping	Wenxian	93.14	0.016	8.16
	Shuangyanwo1#	Pengzhou	73.37	0.07	12.43
	Shuangyanwo2#		75.48	0.063	8.19
	Zhangjia	Beichuan	90.63	0.02	34.75
	Moping	Pingwu	84.81	0.037	10.62
	Wenjia	Mianzhu	97.19	0.006	19.33
	Lower Mozi	Wenchuan	66.62	0.087	23.56
	Upper Mozi		86.35	0.03	101.03
	Lower Niujuan		80.25	0.05	26.44
	Upper Niujuan		89.71	0.025	24.95
	Zoumaling	Mianzhu	85.62	0.037	39.08
Zhouqu, Gansu 2012-08-08 Large debris flows	Luojiayu	ZG (591)	92.83	0.022	26.12
		NSL (N609)	90.93	0.029	13.72
		PJW (GPS613)	90.32	0.040	12.68
		YZG-PJW1# (36)	90.44	0.032	13.75
		PJW 2# (GPS37)	88.68	0.049	23.28
		NSL (GPS:601)	90.94	0.047	9.77
		NSL (GPS:602)	90.58	0.010	13.27
	Sanyanyu	NSL-DJW (GPS55)	87.42	0.048	26.88
		XY-NSL GPS55	96.67	0.006	27.62
		NSL-WY N625	85.27	0.061	36.11
		NSL-WY (GPS625)	85.89	0.052	26.21
		WY (GPS625)	93.55	0.014	23.83
		WY (GPS629)	72.06	0.098	27.77
		XY-NSL (GPS63)	69.36	0.137	15.23
		WY-DY (GPS627)	78.12	0.089	22.06
		XY-NSL (GPS57)	84.96	0.041	29.75

Table 14
GSD parameters of debris flows in Sichuan, 2012.

No.	Area	Location			GSD parameters			
		Gullies	GPS		C	μ	D_c	R^2
SY1	Xichang	North Gully	GPS830	④	86.66	0.0371	25.28	0.9527
SY2		Lower North Gully		⑥	67.79	0.0827	92.02	0.9762
SY3		South Gully	GPS832	⑦	79.02	0.0541	56.24	0.9780
SY4		Tuunel2#	GPS822	②	71.27	0.0651	20.98	0.9960
SY6		Miansha Gully	GPS827	③	61.13	0.1012	22.60	0.9841
SY7		Outlet	GPS831	①	79.26	0.0517	24.58	0.9855
SY8		Dabenliu	GPS821	⑤	91.75	0.0160	44.18	0.9919
SY9	Gaochuan	Dongzi Gully	GPS68	⑤	99.23	0.0033	15.32	0.9891
SY10		Gangou	GPS70		98.86	0.0026	19.30	0.9964
SY11		Xinqiao dam	GPS69		89.05	0.0237	22.09	0.9935
SY12		Ganhe Gully	GPS71	⑪	92.35	0.0138	36.44	0.9794
SY13		Daoxi Gully	GPS11	⑫	82.84	0.0371	19.70	0.9955
SY14		Gaochuan	GPS24		95.36	0.0077	16.47	0.9989
SY15		Xujia Gully	GPS117	21	88.31	0.0317	24.82	0.9675
SY16		Rill flow	GPS31		87.44	0.0284	16.75	0.9975
SY17		Huapa Gully	GPS42	④	94.05	0.0149	26.09	0.9960
SY18			GPS16	⑥	92.87	0.0140	23.32	0.9955
SY40		Sanchadong Gully	GPS67	②	93.92	0.0142	9.58	0.9988
SY44		Shuimo Gully	GPS6	③	86.39	0.0352	14.18	0.9891
SY19	Yinchang Gully, Pengzhou	Outlet	GPS76	⑬	93.09	0.0149	31.35	0.9871
SY20		Xiejiadianzi	GPS95	⑱	90.11	0.0203	23.63	0.9851
SY21		Xiangshuidong	GPS120	⑲	93.59	0.0144	20.12	0.9987
SY22		Gangou Gully	GPS84		91.67	0.0188	26.05	0.9987
SY23		Shuangyanwo	GPS78	⑭	72.11	0.0742	9.78	0.9735
SY24		Guanzi Gully	GPS79	⑮	94.46	0.0136	12.49	0.9988
SY25		Songzidian	GPS119	⑯	82.30	0.0426	39.07	0.9802
SY26		Donglinsi	GPS121	⑳	90.83	0.0241	13.33	0.9939
SY27	Sichuan–Tibet highway	Tributary 3			89.11	0.0258	13.37	0.9930
SY28		Tributary 5			93.23	0.0160	11.05	0.9953
SY29		Right tributary			89.33	0.0240	33.63	0.9927
SY30		Mainstream source			84.95	0.0334	8.14	0.9961
SY31		Right tributary 1	GPS564		93.74	0.0120	26.92	0.9981
SY32		Right tributary 2	GPS565		89.85	0.0191	25.87	0.9923
SY33		Tributary 4			88.51	0.0283	13.02	0.9923
SY34		Deposit 6			97.84	0.0036	10.19	0.9976
SY35			GPS548		88.89	0.0242	16.06	0.9978
SY36		Haitong Gully			91.50	0.0189	14.52	0.9986
SY37	Ya'an	631			84.83	0.0367	21.51	0.9916
SY 5		Dam 2	GPS628	22	89.37	0.0262	15.41	0.9970
SY 38			GPS650		90.86	0.0228	8.01	0.9958
SY 39		Jiaochang Gully	GPS634		81.75	0.0448	12.57	0.9934
SY 45			GPS633	5	77.72	0.0599	22.15	0.9726
SY 42		Lengnu Gully			80.96	0.0487	20.07	0.9839
SY 43		Sanli Gully	GPS630		82.00	0.0449	24.05	0.9910
SY 41	Dujiangyan	Tangfang Gully	GPS590		87.12	0.0314	28.42	0.9941
SY 46			GPS556	①	89.73	0.0250	27.01	0.9960

the observations that debris flows in general have $\mu < 0.10$ and most debris flows of high density have $\mu < 0.05$.

Experiments reveal that μ increases with loss of fine grains, which is accompanied by the increase of porosity. Therefore the GSD provides a quantitative description of changes in grain composition, which is helpful in understanding the material variations during the processes of debris flow developing.

Applying the GSD to debris flows in various regions, we find that the parameter points (μ, D_c) fall into a certain range and present regional distinctions. This can be used as criterion to evaluate historical or potential debris flows in terms of the GSD parameters of the deposit or source soils.

The discussion throughout this study puts emphasis on the integrity of grain composition, claiming that debris flow depends not only on a special ingredient (e.g., the fine content), but also (and much more) on the total feature of the composition, which can be characterized by the distribution we propose here. This suggests that simulating a debris flow should better use natural soil rather than the man-sorted grains so that it can reveal the soil behavior more accurately, especially the variation of parameters in different conditions.

Further problems exist still concerning the findings, among which the most urgent is to explore the relationships between the GSD parameters and the dynamical behaviors of soil, the variation of parameters in the processes of debris flow evolving. Further studies are needed on the variation of soil quantities (e.g., moisture, porosity, pore water pressure, yield strength) with characteristics of soil failures of different GSD parameters, the effect of granular variation in debris flow motion. All these are expected to provide a more detailed and quantitative picture for the formation and evolution of debris flow from various soils.

Acknowledgments

This research is supported by the Key Research Program of the Chinese Academy of Sciences (grant no. KZZD-EW-05-01), the National Natural Science Foundation of China (grant no. 40771010), and the National Key Technology Research and Development Program (grant no. 2012BAK10B04).

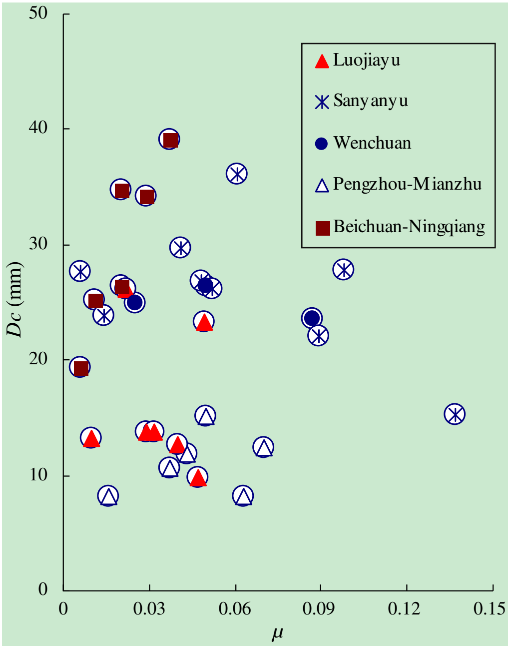

Fig. 16. (μ, D_c) points for debris flows in Wenchuan and Zhouqu.

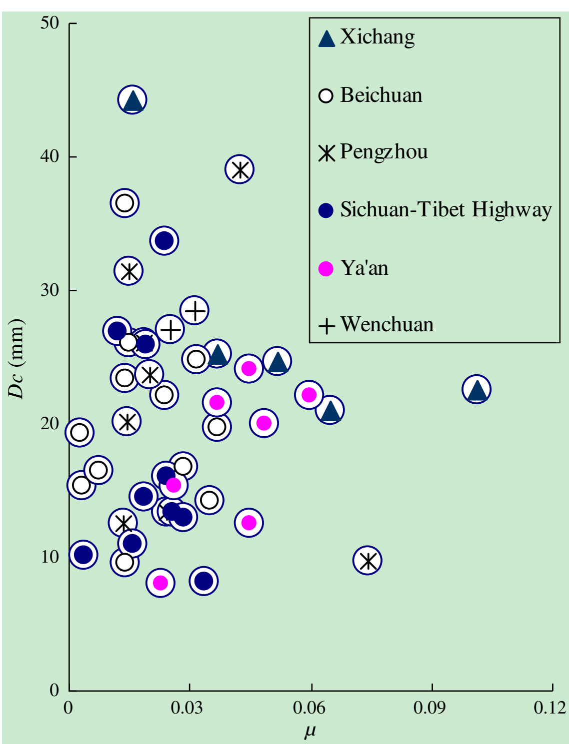

Fig. 17. (μ, D_c) points for debris flows in Sichuan, 2012.

References

Arya, L.M., Paris, J.F., 1981. A physico-empirical model to predict the soil moisture characteristic from particle size distribution and bulk density data. Soil Science Society of America Journal 45, 1023–1080.

Aste, T., Tordesillas, A., Matteo, T.D. (Eds.), 2007. Granular And Complex Materials. Lecture Notes in Complex Systems, vol. 8. World Scientific, Singapore.

Avnir, D., Frain, D., Pfeifer, P., 1985. Surface geometric irregularity of particulate materials: the fractal approach. Journal of Colloid and Interface Science 103, 112.

Bagnold, R.A., 1954. Experiments on a gravity-free dispersion of large solid spheres in a Newtonian fluid under shear. Proceedings of the Royal Society of London Series A 225, 49–63.

Bagnold, R.A., 1956. The flow of cohesionless grains in fluids. Proceedings of the Royal Society of London Series A 249, 235–297.

Bardou, E., Boivin, P., Pfeifer, H.-R., 2007. Properties of debris flow deposits and source materials compared, implications for debris flow characterization. Sedimentology 54, 469–480.

Batrouni, G.G., Dippel, S., Samson, L., 1996. Stochastic model for the motion of a particle on an inclined rough plane and the onset of viscous friction. Physical Review E53 (6), 6496–6503.

Bittelli, M., Campbell, G.S., Flury, M., 1999. Characterization of particle-size distribution in soil with a fragmentation model. Soil Science Society of America Journal 63, 782–788.

Brown, W.K., Wohletz, K.H., 1995. Derivation of the Weibull distribution based on physical principles and its connection to the Rosin–Rammler and lognormal distributions. Journal of Applied Physics 78 (4), 2758–2763.

Buchan, G.D., 1989. Applicability of the simple lognormal model to particle size distribution in soils. Soil Science 147, 155–161.

Buchan, G.D., Grewal, K.S., Robson, A.B., 1993. Improved models of particle size distribution, an illustration of model comparison techniques. Soil Science Society of America Journal 57, 901–908.

Campbell, G.S., 1985. Soil Physics with Basic: Transport Models for Soil-Plant Systems. Elsevier Science Publishing Company, Inc., New York.

Campbell, C.S., 1989. Self-lubrication for long run-out landslides. Journal of Geology 97, 653–665.

Campbell, C.S., 1990. Rapid granular flows. Annual Review of Fluid Mechanics 22, 57–92.

Chen, C.L., 1988. Generalized viscoplastic modeling of debris flow. Journal of Hydraulics Division, ASCE 114 (3), 237–258.

Chen, N.S., Zhou, W., Yang, C.L., Hu, G.S., Gao, Y.C., Han, D., 2010. The processes and mechanisms of failure and debris flow initiation for gravel soil with different clay content. Geomorphology 121, 222–230.

Christiansen, C.C., Hartmann, D., 1988. On using the log-hyperbolic distribution to describe the textural characteristics of eolian sediments: discussion. Journal of Sedimentary Petrology 58 (1), 159–160.

Cleary, P.W., Campbell, C.S., 1993. Self-lubrication for long runout landslides, examination by computer simulation. Journal of Geophysical Research 98 (B12), 21,911–21,924.

Cooke, R.U., Warren, A., Goudie, A.S., 1993. Desert Geomorphology. UCL Press, London.

Costa, J.E., 1984. Physical geomorphology of debris flows. In: Costa, J.E., Fleisher, P.J. (Eds.), Developments and Applications of Geomorphology. Springer-Verlag, Berlin, pp. 268–317.

Coussot, P., 1997. Mudflow Rheology and Dynamics. A.A Balkema Publishers, Rotterdam, Netherlands.

Coussot, P., Ancey, C., 1999. Rheophysical classification of concentrated suspensions and granular pastes. Physical Review E 59, 4445–4457.

Coussot, P., Meunier, M., 1996. Recognition, classification and mechanical description of debris flows. Earth-Science Reviews 40, 209–227.

Cui, P., Chen, X.Q., Zhu, Y.Y., Wei, F.Q., Han, Y.S., Liu, H.J., Zhuang, J.Q., 2011. The Wenchuan Earthquake (May 12, 2008), Sichuan Province, China, and resulting geohazards. Natural Hazards 56 (1), 19–36.

D'Ambrosio, D., Spataro, W., Iovine, G., Miyamoto, H., 2007. A macroscopic collisional model for debris flows simulation. Environmental Modelling & Software 22, 1417–1436.

Das, B.M., 2008. Advanced Soil Mechanics, 3rd ed. Taylor & Francis, London and New York (567 pp).

Fei, X.J., Shu, A.P., 2004. Movement Mechanism and Disaster Control for Debris Flow. Tsinghua University Press, Beijing 41–48 (in Chinese).

Filgueira, R.R., Pachepsky, Y.A., Fournier, L.L., 2003. Time–mass scaling in soil texture analysis. Soil Science Society of America Journal 67, 1703–1706.

Filgueira, R.R., Fournier, L.L., Cerisola, C.I., Gelati, P., Garcia, M.G., 2006. Particle-size distribution in soils: a critical study of the fractal model validation. Geoderma 134, 327–334.

Fink, J.H., Malin, M.C., D'Alli, R.E., Greeley, R., 1981. Rheological properties of mudflows associated with the spring 1980 eruptions of Mount St. Helens volcano, Washington. Geophysical Research Letters 8, 43–46.

Fu, H., Pei, S., Wan, C., Sosebee, R.E., 2009. Fractal dimension of soil particle size distribution along an altitudinal gradient in the Alxa rangeland, western Inner Mongolia. Arid Land Research and Management 23 (2), 137–151.

Gardner, W.R., 1956. Representation of soil aggregate-size distribution by a logarithmic-normal distribution. Soil Science Society of America Journal 20 (2), 151–153.

Gevirtzman, H., Roberts, P.V., 1991. Pore scale spatial analysis of two immiscible fluids in porous media. Water Resources Research 27 (4), 1167–1173.

Gray, J.M.N.T., Kokelaar, B.P., 2010. Large particle segregation, transport and accumulation in granular free-surface flows. Journal of Fluid Mechanics 652, 105–137. http://dx.doi.org/10.1017/S002211201000011X.

Hiscott, R.N., James, N.P., 1985. Carbonate debris flows, Cow Head Group, western Newfoundland. Journal of Sedimentary Petrology 55, 735–745.

Hu, K.H., Ge, Y.G., Cui, P., Guo, X.J., Yang, W., 2010. Preliminary analysis of extra-large-scale debris flow disaster in Zhouqu County of Gansu Province. Journal of Mountain Science 28 (5), 628–634 (in Chinese).

Hungr, O., 1995. A model for the runout analysis of rapid flow slides, debris flows and avalanches. Canadian Geotechnical Journal 32, 610–623.

Hunt, A.G., 2004a. Continuum percolation theory for pressure-saturation characteristics of fractal soils, extension to non-equilibrium. Advances in Water Researches 27, 245–257.

Hunt, A.G., 2004b. Percolation transport in fractal porous media. Chaos, Solitons and Fractals 19, 309–325.
Hunt, A.G., Gee, G.W., 2002. Application of critical path analysis to fractal porous media, comparison with examples from the Hanford site. Advances in Water Resources 25, 129–146.
Hutter, K., Svendsen, B., Rickenmann, D., 1996. Debris flow modeling: a review. Continuum Mechanics and Thermodynamics 8, 1–35.
Hwang II, S., Kwang, P.L., Dong, S.L., Powers, S.E., 2002. Models for estimating soil particle-size distributions. Soil Science Society of America Journal 66, 1143–1150.
Innes, J.L., 1983. Lichenometric dating of debris-flow deposits in the Scottish highlands. Earth Surface Processes and Landforms 8 (6), 579–588.
Iverson, R.M., 1997. The physics of debris flows. Reviews of Geophysics 35 (3), 245–296.
Iverson, R.M., Denlinger, R.P., 1987. The physics of debris flows — a conceptual assessment. In: Beschta, R.L., Blinn, T., Grant, G.E., Ice, G.G., Swanson, F.J. (Eds.), Erosion and Sedimentation in the Pacific Rim. Proceedings of the Corvallis Symposium: Int. Assoc. Hydrol. Sci., Salem, OR, pp. 155–165.
Iverson, R.M., Vallance, J.W., 2001. New views of granular mass flows. Geology 29 (2), 115–118.
Iverson, R.M., Reid, M.E., Iverson, N.R., LaHusen, R.G., Logan, M., Mann, J.E., Brien, D.L., 2000. Acute sensitivity of landslide rates to initial soil porosity. Science 290, 513–516.
Jaeger, H.M., Nagel, S.R., 1992. Physics of the granular state. Science 255, 1523–1530.
Jan, C.D., Shen, H.W., 1997. Review dynamic modeling of debris flows. In: Armanini, A., Michiue, M. (Eds.), Recent Developments on Debris Flows. Springer-Verlag, Berlin-Heidelberg, pp. 93–116.
Johnson, A.M., 1970. Physical Processes in Geology. Freeman, Cooper, and Co, San Francisco (576 pp).
Johnson, A.M., 1984. Debris flow. In: Brunsden, D., Prior, D.B. (Eds.), Slope Instability. John Wiley and Sons, New York, pp. 257–361.
Johnson, C.G., Kokelaar, B.P., Iverson, R.M., Logan, M., LaHusen, R.G., Gray, J.M.N.T., 2012. Grain-size segregation and levee formation in geophysical mass flows. Journal of Geophysical Research 117, F01032. http://dx.doi.org/10.1029/2011JF002185.
Julien, P.Y., Lan, Y.Q., 1991. Rheology of hyperconcentrations. Journal of Hydraulic Engineering 117 (3), 346–353.
Kaitna, R., Rickenmann, D., 2007. Flow of different material mixtures in a rotating drum. In: Chen, C.L., Major, J.J. (Eds.), Debris-flow Hazard Mitigation: Mechanics, Prediction, and Assessment. Millpress, Rotterdam, Netherland, pp. 269–279.
Kaitna, R., Rickenmann, D., Schatzmann, M., 2007. Experimental study on the rheologic behaviour of debris flow material. Acta Geotechnica 2 (2), 71–85.
Katz, A.J., Thompson, A.H., 1985. Fractal sandstone pores, implications for conductivity and pore formation. Physical Review Letters 54 (12), 1325–1328.
Kim, S.B., Chough, S.K., Chun, S.S., 1995. Bouldery deposits in the lowermost part of the Cretaceous Kyokpori Formation, SW Korea: cohesionless debris flows and debris falls on a steep-gradient delta slope. Sedimentary Geology 98, 97–119.
Kittleman, L.R., 1964. Application of Rosin's distribution in size frequency analysis of clastic rocks. Journal of Sedimentary Petrology 34, 483–502.
Li, Y., Chen, X.Q., Hu, K.H., He, S.F., 2005. Fractality of grain composition of debris flows. Journal of Geographical Sciences 15 (3), 353–359.
Li, Y., Liu, J.J., Hu, K.H., Su, P.C., 2012. Probability distribution of measured debris-flow velocity in Jiangjia gully, Yunnan Province, China. Natural Hazards 60 (2), 689–701.
Liu, J.J., Li, Y., Su, P.C., Cheng, Z.L., 2008. Magnitude-frequency relations in debris flows. Environmental Geology 55, 1345–1354.
Liu, J.J., Li, Y., Su, P.C., Cheng, Z.L., Cui, P., 2009. Temporal variation of intermittent surges of debris flow. Journal of Hydrology 365 (3–4), 322–328.
Nemec, W., Steel, R.J., 1984. Alluvial and coastal conglomerates, their significant features and some comments on gravelly mass-flow deposits. In: Koster, E.H., Steel, R.J. (Eds.), Sedimentology of Gravels and Conglomerates: Canadian Society of Petroleum Geologists, Memoir, 10, pp. 1–31 (Calgary, Alberta, Canada).
Nimmo, J.R., Herkelrath, W.N., Luna, A.M., 2007. Physically based estimation of soil water retention from textural data: general framework, new models, and streamlined existing models. Vadose Zone Journal 6 (4), 766–773. http://dx.doi.org/10.2136/vzj2007.0019.
Pachepsky, Y.A., Polubesova, T.A., Hajnos, M., Sokolowska, Z., Jouzefaciuk, G., 1995. Fractal parameters of pore surface area as influenced by simulated soil degradation. Soil Science Society of America Journal 59, 68–75.
Pachepsky, Y., Crawford, J.W., Rawls, W.J., 2000. Fractals in Soil Science. Reprinted from Geoderma 88, 3–4 Elsevier, Amsterdam (294 pp).
Perfect, E., Kay, B.D., 1991. Fractal theory applied to soil aggregation. Soil Science Society of America Journal 55, 1552–1558.
Perfect, E., Rasiah, V., Kay, B.D., 1992. Fractal dimensions of soil aggregate-size distributions calculated by number and mass. Soil Science Society of America Journal 56, 1407–1409.
Pinnick, R.G., Fernandez, G., Hinds, B.D., Bruce, C.W., Schaefer, R.W., Pendleton, J.D., 1985. Dust generated by vehicular traffic on unpaved roadways: sizes and infrared extinction characteristics. Aerosol Science and Technology 4, 99–121.
Rieu, M., Sposito, G., 1991. Fractal fragmentation, soil porosity, and water properties: I. Theory. Soil Science Society of America Journal 55, 1231.
Schofield, A., Wroth, P., 1968. Critical State Soil Mechanics. McGraw-Hill, London (310 pp).
Shirazi, M.A., Boersma, L., 1984. A unifying quantitative analysis of soil texture. Soil Science Society of America Journal 48 (1), 142–147.
Su, P.C., Wei, F.Q., Cheng, Z.L., 2011. Debris flows in Mozi gully, China, following the 2008 Wenchuan earthquake. Proceeding of the 5th International Conference on Debris-Flow Hazards Mitigation: Mechanics, Prediction and Assessment, Padova, Italy, 14–17 June 2011. Casa Editrice Università La Sapienza, Rome, Italy, pp. 769–777.
Tang, C., Rengers, N., Van Asch, T.W.J., Yang, Y.H., Wang, G.F., 2011. Triggering conditions and depositional characteristics of a disastrous debris-flow event in Zhouqu city, Gansu Province, northwestern China. Natural Hazards and Earth System Sciences 11 (11), 2903–2912.
Turcotte, D.L., 1986. Fractals and fragmentation. Journal of Geophysical Research 91, 1921–1926.
Tyler, S.W., Wheatcraft, S.W., 1992. Fractal scaling of soil particle size distributions, analysis and limitations. Soil Science Society of America Journal 56, 362–369.
Wagner, L.E., Ding, D.J., 1992. Modeling tillage actions on soil aggregates. ASAE, Paper No. 92-2133, pp. 49085–49659. St. Joseph, MI.
Wohletz, K.H., Sheridan, M.F., Brown, W.K., 1989. Particle size distributions and sequential fragmentation/transport theory applied to volcanic ash. Journal of Geophysical Research 91 (B11), 15703–15721.
Wu, J.S., Kang, Z.C., Tian, L.Q., Zhang, S.C., 1990. Observation Research of Debris Flows in Jiangjia Gully. Yunnan. Science Press, Beijing (251 pp).
Yu, B., Yang, Y.H., Su, Y.C., Huang, W.J., Wang, G.F., 2010. Research on the giant debris-flow hazards in Zhouqu county, Gansu Province on August 7 2010. Journal of Engineering Geology 4, 437–444 (in Chinese).
Zhou, X.J., Cui, P., Li, Y., 2012. Flume test study on the movement of fine grains based on orthogonal design. Journal of Sichuan University (Engineering Science Edition) 44 (s1), 83–89 (in Chinese).